# Rabaptin4, a novel effector of the small GTPase rab4a, is recruited to perinuclear recycling vesicles

Bas NAGELKERKEN, Eelco VAN ANKEN, Marcel VAN RAAK, Lisya GEREZ, Karin MOHRMANN, Nathalie VAN UDEN, Jessica HOLTHUIZEN, Lucas PELKMANS and Peter VAN DER SLUIJS[1]

Department of Cell Biology, Utrecht University School of Medicine, Heidelberglaan 100, 3584 CX Utrecht, The Netherlands

The small GTPase rab4a is associated with early endocytic compartments and regulates receptor recycling from early endosomes. To understand how rab4a mediates its function, we searched for proteins which associate with this GTPase and regulate its activity in endocytic transport. Here we identified rabaptin4, a novel effector molecule of rab4a. Rabaptin4 is homologous with rabaptin5 and contains a C-terminal deletion with respect to rabaptin5. Rabaptin4 preferentially interacts with rab4a–GTP and to a lesser extent with rab5aGTP. We identified a rab4a-binding domain in the N-terminal region of rabaptin4, and two binding sites for rab5, including a novel N-terminal rab5a-binding site. Rabaptin4 is a cytosolic protein that inhibits the intrinsic GTP hydrolysis rate of rab4a and is recruited by rab4a–GTP to recycling endosomes enriched in cellubrevin and internalized indocarbocyanine-3 (Cy3)-labelled transferrin. We propose that rabaptin4 assists in the docking of transport vesicles en route from early endosomes to recycling endosomes.

Key words: endocytosis, small G protein, transferrin receptor, recycling endosomes.

## INTRODUCTION

Rab proteins constitute the largest subfamily (> 35 members) of the ras family of small GTPases and are involved in the regulation of vesicular transport [1]. How rab proteins participate in docking and fusion of transport vesicles is not fully understood. Rab proteins are thought to interact with downstream effectors that specifically recognize their GTP-bound conformation [2]. These and possibly other proteins are then recruited on a vesicle and may play a role in the stabilization of a soluble NSF attachment protein receptor (SNARE) complex on vesicle docking. In this model rab proteins exert spatio-temporal control on the activity of SNARE complexes. Several rab effector proteins were recently identified, including rim [3], p40 [4], rabaptin5 [5], early endosome-associated antigen 1 (EEA1) [6], rab8ip [7], and rab6kinesin [8]. Perhaps the best characterized rab effector is rabaptin5. This cytosolic protein is required for homotypic early endosome fusion and interacts with rab5aGTP and rabex5 [9]. The specificity of rabaptin5 is not limited to rab5a, since it also contains a binding site for rab4a [10]. The significance of the rab4a-binding site, however, has not been addressed so far, nor has the intracellular location where this interaction occurs. Once recruited on rab5aGTP, rabaptin5 is thought to stabilize this conformation by antagonizing the activity of a GTPase-activating protein (GAP), until docking has been completed [11].

Several rab proteins are functionally associated with early endocytic organelles. Rab5a regulates the uptake of solute and receptor-bound ligands from the cell surface via clathrin-coated vesicles [12]. Rab11 is localized to the recycling endosomes and the *trans*-Golgi network, where it regulates recycling of membrane receptors [13] and exocytosis to the plasma membrane [14]. Rab4a is associated with early endosomes and recycling vesicles [15], and *in vivo* regulates exit of the transferrin receptor (TfR) from the early endosome [16]. *In vitro*, rab4a stimulates fission of, or budding from early endosomes that are formed in a rab5a-dependent homotypic fusion assay [17], and the formation of transferrin (Tf) containing recycling vesicles (H. de Wit, Y. Liechtenstein, R. Kelly, J. Klumperman and P. van der Sluijs, unpublished work), suggesting that rab5a and rab4a co-ordinately regulate early-endosome membrane dynamics [17].

To investigate how GTP-hydrolysis on rab4a is related to the function of this protein in endocytosis, we searched for its downstream effectors. We identified rabaptin4, a protein that is related to rabaptin5. Rabaptin4 is recruited by rab4a to the perinuclear region where it co-localized with internalized Tf and cellubrevin. Since we found that rabaptin4 binds rab4a–GTP on recycling endosomes, our results suggest a role for rab4a and rabaptin4 in transport from early endosomes to recycling endosomes.

## MATERIALS AND METHODS

### Antibodies

Affinity-purified rabbit antibodies against rab4a [18], cellubrevin [19], and the mouse monoclonal against the X31 influenza haemagglutinin NH epitope tag [20], were characterized in the indicated references. The anti-Xpress mouse monoclonal was

Abbreviations used: EEA1, early endosome-associated antigen 1; CHO, Chinese-hamster ovary; Cy3, indocarbocyanine-3; DABCO, 1,4-diazobicyclo[2.2.2]octane; DTSP, dithiobis(succinimidyl propionate); GAP, GTPase-activating protein; GBD, GAL4 binding domain; Ni-NTA, $Ni^{2+}$-nitrilotriacetate; NSF, *N*-ethylmaleimide-sensitive factor; RACE, rapid amplification of cDNA ends; RT, reverse transcriptase; SNARE, soluble NSF attachment protein receptor; Tf, transferrin; TfR, transferrin receptor

[1] To whom correspondence should be addressed (e-mail pvander@knoware.nl).

The nucleotide sequence of rabaptin4 gene has been submitted to the GenBank, DDBJ and EMBL Nucleotide Sequence Databases under the accession number AF098638.

from Invitrogen (San Diego, CA, U.S.A.) and fluorescently-labelled secondary antibodies were from Jackson Immunoresearch Laboratories (West Grove, PA, U.S.A.).

### Plasmids

cDNAs encoding rab2, rab4a, rab4b, rab5a, rab6, rab7, rab4aQ67L, rab4aS22N and rab5aQ79L were inserted in pGBT9 (ClonTech–Westburg, Leusden, The Netherlands). The plasmids pGBT8-rap1aG12V and pGADGH-ralGDS-RBD have been described before [21]. cDNAs encoding clone #16B (amino acid residues 11–830), rabaptin4ΔC (amino acid residues 11–388), rabaptin4ΔN (amino acid residues 469–830), and rabaptin5ΔN (amino acid residues 469–863) were inserted in pGADGH (ClonTech–Westburg) and pcDNA3.1/His (Invitrogen, Leek, The Netherlands). Full-length rabaptin4 and rabaptin5 were inserted in pcDNA3 (Invitrogen, Leek, The Netherlands). pRSET-A-rab4a [18], and pRSET-C-rabaptin4ΔC (Invitrogen) were used for production of His-tagged fusion proteins in *Escherichia coli*. cDNA generated in PCR reactions was verified by dideoxy sequencing.

### Yeast two-hybrid screening

The yeast reporter strain YGH1 (ClonTech–Westburg) was co-transformed with pGBT9-rab4aQ67L and a HeLa cell oligo(dT)-primed cDNA library in pGADGH. Colonies were tested for $\beta$-galactosidase activity using a replica filter assay. Liquid $\beta$-galactosidase assays were done on at least three colonies of each transformation and the activity of transformants was normalized to that of the full-length GAL4 transcriptional activator in pCL1 (Clontech–Westburg).

### Miscellaneous nucleic acid methods

RNA was reverse-transcribed and cDNA amplified using the oligonucleotides 5′-CTC-TGC-AAC-TAG-TAA-TAG-AAA-ACT-G-3′ and 5′-TCA-TTC-AGA-ATT-GCC-CGG-ATT-CTC-TCC-3′. Genomic HeLa cell DNA was amplified using the same primers. The 5′ end of rabaptin4 was generated by 5′ rapid amplification of cDNA ends (RACE) using specific primers, 5′-GTGTTCGCTCCTGCTCCAGC-3′, 5′-GCTTCCCACAGCT-GGGTTCG-3′, 5′-GGTTCGAAGGTGTCCCAAATCATC-3′. PCR reactions were run in triplicate and products were cloned in pGEM-T (Promega) and analysed by dideoxynucleotide chain-termination.

### *In vitro* binding assay

Recombinant rab4a and rabaptin4ΔC (amino acid residues 11–388) were produced as His-fusion proteins in *E. coli* BL21(DE3)pLysS. Fusion proteins were stored at −80 °C in 50 mM K-Pipes, pH 8.0, 150 mM KCl, 1 mM EDTA, 0.5 mM $MgCl_2$, 1 mM dithiothreitol (DTT), 0.1 % CHAPS (buffer A). *In vitro* binding of His-rab4a to His-rabaptin4ΔC was assayed in microtitre plates. Wells were coated with 300 ng of His-rabaptin4ΔC in 100 mM $Na_2CO_3$, pH 9.5, blocked with Blotto [5 % (w/v) milk in TBST (10 mM Tris/HCl, pH 8.0, 150 mM NaCl, 0.05 % (v/v) Tween 20)] and washed five times with Blotto between incubations. His-rab4a was added in 5 mM $MgCl_2$, 1 mM GDP or GTP in TBST and incubated for 1 h at room temperature. His-rab4a was detected with anti-rab4a antibodies followed by horseradish peroxidase-conjugated goat anti-rabbit antibodies, and assayed colorometrically at 450 nm.

### GTPase- and GDP/GTP exchange assays

Rab4a GTPase activity was assayed using charcoal precipitation [22]. Reactions were carried out at 37 °C in buffer A containing 200 nM active His-rab4a, 500 nM [$\gamma$-$^{32}$P]GTP ($7.4 \times 10^{11}$ Bq/mmol), and 2 $\mu$M His-rabaptin4ΔC or BSA (control). Timed aliquots were mixed with 750 $\mu$l of 5 % activated charcoal in 50 mM $NaH_2PO_4$ on ice, and centrifuged at 3000 ***g*** for 10 min at 4 °C. Released [$^{32}$P]$P_i$ was quantified by liquid-scintillation counting. Guanine nucleotide exchange was measured using a filter-binding assay. His-rab4 was charged for 2 h at 30 °C in buffer A containing 1.3 mM GDP. The reaction mixture was immediately passed through a PD10 column (Pharmacia) and eluted with buffer A at 4 °C to remove non-bound GDP. His-rab4aGDP (50 nmol) was subsequently incubated with 1 $\mu$M [$^{35}$S]guanosine 5′-[$\gamma$-thio]triphosphate ($3.7 \times 10^6$ Bq/mmol) at 30 °C in the presence or absence of a 10-fold molar excess of His-rabaptin4ΔC. Timed duplicate aliquots of 20 $\mu$l were retrieved, diluted with 2 ml of ice-cold 20 mM Tris/HCl (pH 8.0)/150 mM NaCl/1 mM DTT and passed through prewashed Millipore GS 0.22-$\mu$m pore-size filters. Filters were washed twice with ice-cold 20 mM Tris/HCl (pH 8.0)/150 mM NaCl/1 mM DTT, dried, and subjected to liquid-scintillation counting.

### Cell culture and transfection

A His-rabaptin4/rab4a cell line was generated by transfecting pcDNA3.1/His-rabaptin4 into rab4aCHO cells [16] and maintained in media containing 0.6 mg/ml G418 (Geneticin) and 50 $\mu$M methotrexate. Chinese-hamster ovary (CHO) cells were transfected with pcDNA3.1/His-rabaptin4 and either pcDNA3-NHrab4aS22N, pcDNA3-NHrab4aQ67L, pcDNA3-NHrab5a, or pcDNA3-NHrab5aQ79L.

### Co-precipitation of rab4a and His-rabaptin4 on Ni-NTA resin

Both transfected and non-transfected CHO cells were transiently transfected with pCB6-NH-rab4a. After 48 h, the cells were broken in 100 mM Hepes (pH 7.4)/0.1 mM GTP/1 mM $MgCl_2$/50 mM NaF/1 mM PMSF by passing them ten times through a 25-gauge needle. Homogenates were spun for 10 min at 600 ***g*** to prepare a post-nuclear supernatant. The post-nuclear supernatant was then incubated with $Ni^{2+}$-nitrilotriacetate (Ni-NTA) beads (Qiagen–Westburg) by end-over-end rotation for 1 h at 4 °C to collect His-rabaptin4–rab4a complexes. Resin fractions were washed four times with 150 mM NaCl, 100 mM Tris/HCl, pH 8.3, 0.1 % SDS, 0.5 % deoxycholate, 0.5 % Nonidet P40 (RIPA buffer) and boiled in reducing Laemmli sample buffer. Samples were resolved by SDS/PAGE, transferred to PVDF membranes and analysed by Western blotting using the anti-Xpress antibody to detect His-rabaptin4 and a rabbit antibody against rab4a. Quantification was done with Scion Image 1.0 for Windows (Meyer Instruments Inc., Houston, TX, U.S.A.).

### Cross-linking experiments

CHO cells stably transfected with His-rabaptin4, or non transfected CHO cells were transiently transfected with pCB6-NH-rab4a. After 48 h, the dishes were transferred to ice and washed twice with serum-free medium. The cells were then incubated with 0.05 % (w/v) saponin, 100 mM Hepes pH 7.4, 0.1 mM GTP, 1 mM $MgCl_2$ on ice. After 30 min, the extraction buffer was aspirated and cells were incubated in the same buffer containing 1 mM dithiobis(succinimidyl propionate) (DTSP) (Pierce BV, Oud Beijerland, The Netherlands) on ice. After 30 min, DTSP was quenched with 20 mM Tris/HCl, pH 7.4, and the cells were homogenized as described above. Post-nuclear super-

natants were then incubated with Ni-NTA beads by end-over-end rotation for 1 h at 4 °C to collect the His-rabaptin4–rab4a complexes. Resin fractions were washed four times with RIPA buffer and split into two aliquots. One aliquot was boiled in reducing sample buffer and the other in non-reducing sample buffer. Samples were resolved by SDS/PAGE on 12.5 % minigels, transferred to PVDF membranes and analysed by Western blotting using anti-Xpress to detect His-rabaptin4, and a rabbit antiserum to detect rab4a.

### Internalization of Cy3-Tf and confocal immunofluorescence microscopy

Human Tf was saturated with $FeCl_3$ as described [16] and labelled with indocarbocyanine-3 (Cy3) according to the vendor's instructions (Amersham). Cells were grown on 11 mm round coverslips to 60 % confluency and for uptake experiments incubated with 25 $\mu$g/ml of Cy3-Tf at 37 °C. After 60 min the coverslips were transferred to ice and surface-bound Cy3-Tf was removed by alternating acid and neutral washes [16]. Coverslips were fixed in 3 % paraformaldehyde for 1 h. After quenching in 50 mM $NH_4Cl$, PBS for 5 min, the cells were permeabilized and blocked for 30 min in 0.1 % saponin, 0.5 % bovine serum albumin in PBS (blocking buffer) and incubated with primary antibodies. The coverslips were washed for three periods of 15 min in blocking buffer and then incubated for 30 min with appropriate combinations of fluorescently-labelled secondary antibodies diluted in blocking buffer. The coverslips were mounted in Moviol containing 2.5 % (w/v) 1,4-diazobicyclo[2.2.2]octane (DABCO) and examined with a 63× Planapo objective on a Leitz DMIRB fluorescence microscope (Leica, Voorburg, The Netherlands) interfaced with a Leica TCS4D confocal laser microscope (Leica Lasertechnik, Heidelberg, Germany) using the following filters: FITC, $\lambda_{excitation} = 488$ nm and $\lambda_{emission} = 520$ nm band pass; and Cy3, $\lambda_{excitation} = 568$ nm and $\lambda_{emission} =$ 590 nm long pass. Images were imported in Adobe Photoshop 4.0.1 (Adobe Systems, San José, CA, U.S.A.) and printed on a Tektronix (Amsterdam, The Netherlands) 450 EF dye-sublimation printer.

## RESULTS

### Identification of rab4a-interacting proteins

To identify rab4a effector proteins, we screened an oligo(dT)-primed two-hybrid HeLa cDNA library with the GTP-hydrolysis-deficient mutant rab4aQ67L. About $1 \times 10^6$ transformants were screened, of which 99 clones grew on selective medium lacking histidine, and activated the $\beta$-galactosidase reporter gene. Library plasmids were recovered and retransformed into YGH1. Eight clones retained the ability to activate $\beta$-galactosidase and one of them, clone #16B, is characterized here.

### #16B specifically interacts with rab4a

To analyse whether #16B interacted specifically with rab4a–GTP, we transformed it into YGH1 strains expressing the GAL4 binding-domain (GBD), GBD-rab4a, GBD-rab4aS22N, GBD-rab4b, GBD-rab2, GBD-rab5a, GBD-rab5aQ79L, GBD-rab6, GBD-rab7 and GBD-rap1aG12V. As shown in the left panel of Figure 1, #16B interacted with rab4a and rab4aQ67L, but not with the GDP-bound mutant rab4aS22N, or most of the other GTPases tested, including rab11Q70L (results not shown). A weak activation was also seen with the rab4b isoform. As rab4a and rab5a are associated with early endosomes, we investigated whether rab5aQ79L and rab5a bound to #16B. The GTPase-deficient mutant rab5aQ79L readily interacted with #16B, although to a lesser extent than rab4aQ67L, whereas we did not find reporter activation with wild-type rab5a. A similar difference between rab5a and rab5aQ79L interaction towards rabaptin5 also has been reported by others [5]. Thus #16B encoded a candidate cDNA product specifically interacting with the GTP-bound forms of rab4a and rab5a.

### Identification of rabaptin4

BLAST searches showed that #16B was homologous with rabaptin5 [5]. Compared with rabaptin5, #16B contains an in-frame deletion of 99 bp after position 2271, resulting in the loss of amino acid residues 758–790. Furthermore, the following substitutions were found with respect to the rabaptin5 cDNA: $Cys^{1509} \rightarrow$ Thr, G2286A, C2307T, and A2358G, none of which, however, altered the amino acid sequence. As #16B is not a splice-variant of rabaptin5 (see below), we named it rabaptin4. A full-length rabaptin4 cDNA was generated with 5′ RACE which extended the #16B cDNA by 103 nt including a Kozak, translation-initiation sequence 30 nt upstream of its 5′ end. The predicted coding region of rabaptin4 consists of 2487 bp, encoding a protein of 829 residues with a calculated $M_r$ of 95 561. Sequence alignment with rabaptin5 and rabaptin5$\beta$ showed an identical 33-amino acid deletion in rabaptin5$\beta$. The overall sequence similarity with rabaptin5$\beta$, however, is low, due to sequence divergence at the N-terminus (right panel of Figure). Analysis of the rabaptin4 amino acid sequence with the COILS program [23] suggested that rabaptin4 has the propensity to form extensive $\alpha$-helical coiled-coils in the N- and C-terminal regions. Importantly, the probability to form coiled-coils precipitously decreased beyond the internal deletion (results not shown) when compared with rabaptin5, suggesting that the deletion in rabaptin4 probably conferred conformational changes in the C-terminus of the protein.

### Rabaptin4 is ubiquitously expressed

Since rab4a is expressed in all tissues examined thus far, we next determined the expression pattern of rabaptin4. On Western blots and by immunoprecipitation, rabaptin antibodies detected a single band containing both rabaptin4 and rabaptin5 (results not shown). We therefore devised a duplex reverse transcriptase-PCR assay with primers annealing at 98 nt upstream and 176 nt downstream of the deletion in rabaptin4. For rabaptin4 this assay would produce a 275 bp fragment, whereas amplification of this part of rabaptin5 was predicted to yield a 374 bp fragment. This region in rabaptin5$\beta$ has too low an identity for the primers to anneal and therefore would not be amplified. As shown in Figure 2, we obtained the predicted 275 bp and 374 bp bands from several human cell lines that, on sequencing, were identical with the corresponding regions of rabaptin4 and rabaptin5 respectively. We therefore concluded that both rabaptins are expressed in the same cells, and that #16B was not an artifact of the two-hybrid cDNA library that we used. To investigate whether rabaptin4 and rabaptin5 are generated by alternative splicing, we isolated genomic DNA from HeLa cells and analysed the presence of rabaptin4 and rabaptin5 using the PCR assay. Again, the same two bands were generated as in PCR reactions using cDNA as template as shown in Figure 2. Sequence analysis of the amplified genomic fragments confirmed their identities with each of the rabaptins. Since we did not amplify intron sequences from genomic DNA, rabaptin4 and rabaptin5 did not arise from alternative splicing. Apparently rabaptin4 is less abundant than rabaptin5, although we cannot exclude the possibility that the 374 bp rabaptin5 band also represented

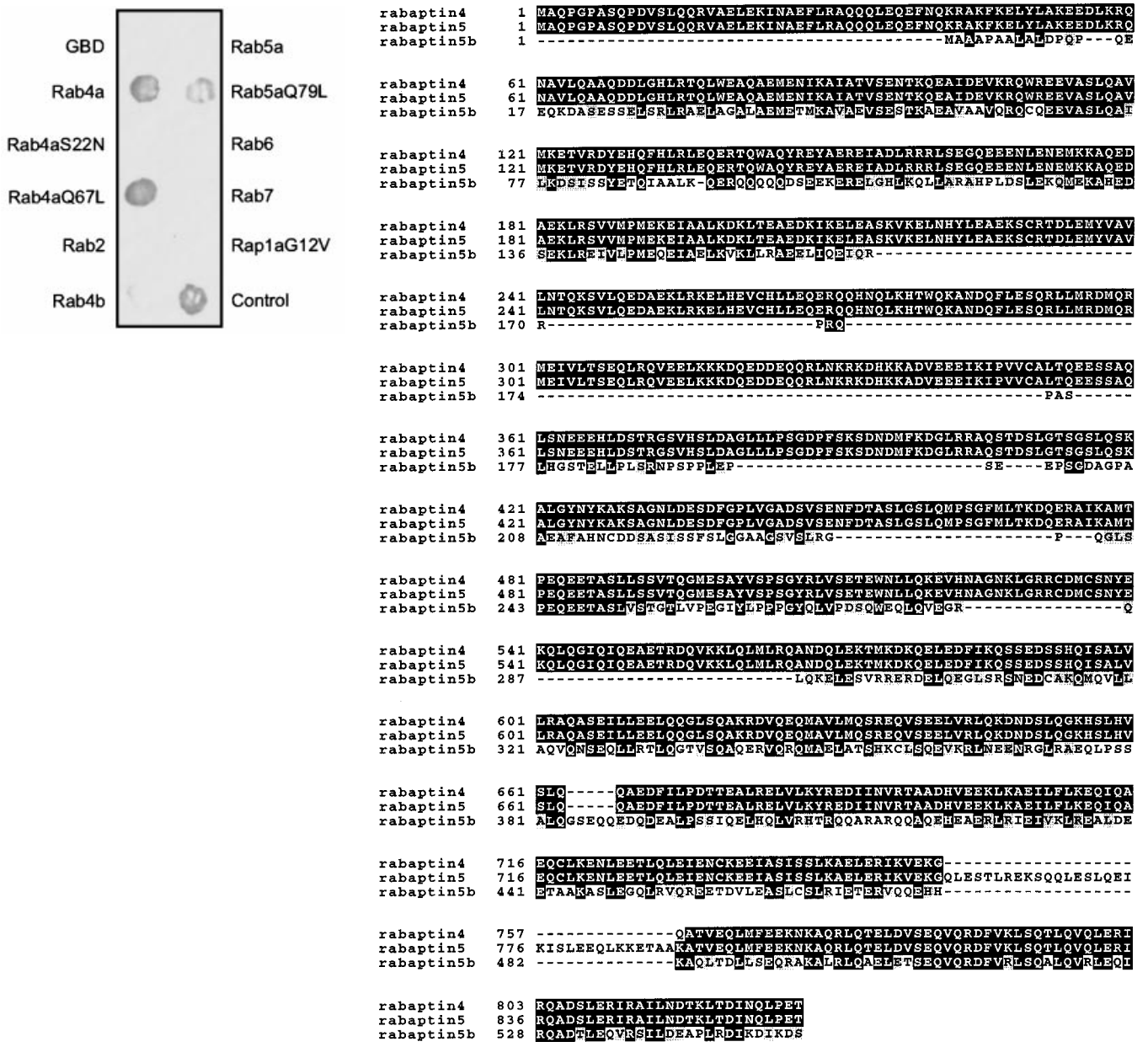


**Figure 1 Identification of #16B as a rab4a effector**

$\beta$-Galactosidase reporter activation of YGH1 cells co-transformed with pGADGH#16B and the indicated cDNAs. As positive control we used rap1aG12V and its partner RalGDS-RBD (left panel). ClustalW alignment of the amino acid sequences of human rabaptin5, human rabaptin4 and mouse rabaptin5$\beta$ showing the identical deletion in rabaptin4 and rabaptin5$\beta$ as compared with rabaptin5 in the C-terminal region (right panel).

amplification products derived from other, as yet unidentified, rabaptins. So far none of the genomic rabaptin DNA sequences are available; we therefore do not know how the identical deletions in rabaptin5$\beta$ and rabaptin4 are generated at present. Rab4a was also amplified from the cDNA of the different cell lines (Figure 2), consistent with the notion that rabaptin4 is an effector of rab4a.

### Rabaptin4 is recruited by rab4a to recycling endosomes

To extend the two-hybrid-system results, we next investigated the localization of rabaptin4 in CHO cells co-expressing His-rabaptin4 and rab4a. Its sequence suggested that rabaptin4 is a hydrophilic protein and, as shown in Figure 3(a), the protein is predominantly localized in the cytoplasm of cells transfected with His-rabaptin4. Western-blot analysis of membrane and cytosol fractions prepared from His-rabaptin4-transfected cells confirmed that rabaptin4 is predominantly a cytosolic protein (results not shown). In His-rabaptin4/NHrab4aQ67LCHO cells, essentially all His-rabaptin4 had disappeared from the cytoplasm and now was concentrated on a perinuclear compartment that also contained NHrab4aQ67L (Figure 3b). These aciniform structures had the appearance of aggregated swollen endosomes, reminiscent of those seen in NHrab4aQ67L CHO single

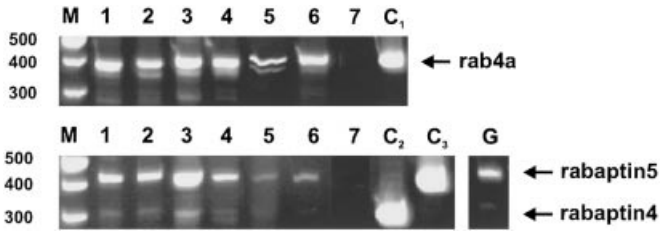


**Figure 2 Expression of rabaptin4**

Rabaptin4 is ubiquitously expressed in human cell lines together with rab4a as analysed by RT-PCR using primers surrounding the deletion in rabaptin4. The same primer-set was also used to document the presence of the rabaptin4 sequence in genomic DNA. As positive controls we included the products obtained using rab4a, full-length rabaptin4, and rabaptin5 cDNAs as template. M, size markers; 1, RN cells; 2, Caco-2 cells; 3, A431 cells; 4, HeLa cells; 5, HepG2 cells; 6, SK-N-MC cells; 7, mock reaction; C1, rab4a cDNA control; C2, rabaptin4 cDNA control; C3, rabaptin5 cDNA control; G, genomic DNA template.

transfectants (Figure 3c). A similar phenotype was seen in His-rabaptin4/rab4aCHO cells (Figure 3d), but not in His-rabaptin4/NHrab4aS22N transfectants (not shown). The fact that co-expression of His-rabaptin4 with either NHrab4aQ67L or rab4a, resulted in the appearance of the perinuclear labelling, strongly suggested a functional interaction between rab4a–GTP and His-rabaptin4 *in vivo* and documented the rab4a-dependent recruitment of rabaptin4 from the cytoplasm to rab4a compartments. The perinuclear structure seen in His-rabaptin4/rab4a cells is a *bona fide* endocytic compartment, since it was accessible to internalized Cy3-Tf and accumulated the tracer when internalized to steady state, as shown in Figure 3(e). His-rabaptin4 also co-localized with NHrab5a (Figure 3f) and NHrab5aQ79L (results not shown). Unlike rab4a, which recruited His-rabaptin4 to perinuclear endosomes, NHrab5a recruited His-rabaptin4 to peripherally localized endosomes in the cytoplasm. The perinuclear organelle on which His-rabaptin4 was recruited by rab4a was also highly enriched in the recycling compartment marker cellubrevin (Figure 3g) and devoid of the Golgi protein GM130 (results not shown). Because rabaptin4 diminishes the intrinsic GTP-hydrolysis rate of rab4a (see below), it might stabilize rab4a on its target compartment from which it otherwise would dissociate upon GTP-hydrolysis. In His-rabaptin4/NHrab5a transfectants (Figure 3h), a significant fraction of cellubrevin co-localized with His-rabaptin4 on peripheral endosomes. In these cells, the perinuclear structure labelled with cellubrevin, however, was devoid of His-rabaptin4 (Figure 3h). This functional *in vivo* immune fluorescence assay for the first time showed the unique abilities of rab4a and rab5a to direct an effector protein to distinct intracellular compartments depending on the local availability of either rab4a–GTP or rab5aGTP.

### Rabaptin4 binds to rab4a *in vivo*

Having shown that co-expression of rab4a and His-rabaptin4 caused the recruitment of His-rabaptin4 from the cytoplasm to

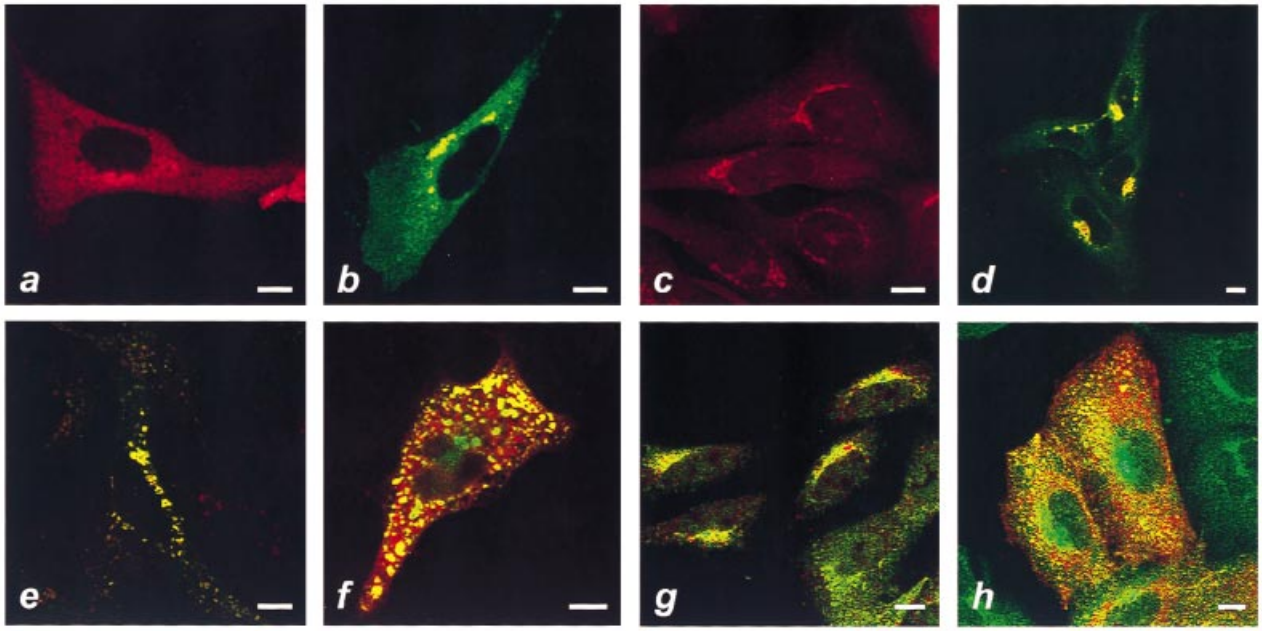


**Figure 3 Subcellular distribution of rabaptin4**

In CHO cells transfected with His-rabaptin4, His-rabaptin4 (red) predominantly shows a diffuse cytosolic labelling (**a**). In His-rabaptin4/NHrab4aQ67L transfectants, His-rabaptin4 (red) and NHrab4aQ67L (green) co-localized on aciniform organelles in the perinuclear region (**b**). In NHrab4aQ67LCHO cells, NHrab4aQ67L (red) localized to a tubulo-vesicular compartment in the perinuclear area (**c**). In CHO cells co-transfected with His-rabaptin4 (red) and rab4a (green) a similar distribution of His-rabaptin4 was observed as in the His-rabaptin4/NHrab4aQ67L transfectant (**d**). When internalized for 60 min at 37 °C in CHO cells expressing His-rabaptin4 (green) and rab4a, Cy3-Tf (red) is found in structures reminiscent of the perinuclear compartment on which rab4a and rabaptin co-localize (**e**). In cells co-transfected with His-rabaptin4 (red) and NHrab5a (green), His-rabaptin4 is recruited to peripherally localized NHrab5a-containing endosomes (**f**). In His-rabaptin4/rab4a transfectants, His-rabaptin4 (red) extensively co-localized with cellubrevin (green) in the perinuclear area (**g**). In CHO cells transfected with rab5a and His-rabaptin4 (red), His-rabaptin4 co-localized with cellubrevin (green) on structures in the peripheral cytoplasm, but not on the distinct cellubrevin compartment adjacent to the nucleus (**h**). Bars represent 10 $\mu$m.

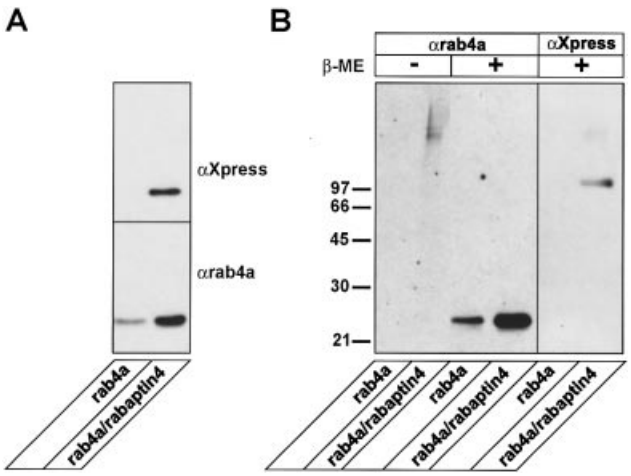


**Figure 4 Interaction between rab4a and His-rabaptin4 *in vivo***

A rab4a CHO cell line was either mock-transfected or transfected with pcDNA3.1/His-rabaptin4. Post-nuclear supernatants were incubated with Ni-NTA resin to bind His-rabaptin4. Resin fractions were washed with RIPA buffer and resolved by SDS/PAGE on 12.5% gels under reducing conditions followed by Western blotting using antibodies against rab4 and His-rabaptin4 (**A**). CHO cells expressing His-rabaptin4 were either mock-transfected or transfected with pCB6-NH-rab4a. Cells were permeabilized with 0.05% saponin and incubated on ice with 1 mM DTSP. Post-nuclear supernatants were incubated with Ni-NTA beads. Fractions bound to the beads were washed with RIPA buffer, resolved on SDS/12.5%-PAGE under non-reducing and reducing conditions, and analysed as described in panel A (**B**).

rab4a-containing endosomes and the expansion of this compartment, we next investigated whether His-rabaptin4 was associated with rab4a *in vivo*. We therefore transfected His-rabaptin4 in a stable rab4a CHO transfectant, to isolate putative complexes containing both proteins. Post-nuclear supernatants of control cells transfected with rab4a, and of His-rabaptin4/rab4a double transfectants, were incubated with Ni-NTA resin to bind the His-rabaptin4 fusion protein. Incubation mixtures were then washed with RIPA buffer and resolved by SDS/12.5 %-PAGE, followed by Western blotting using a rab4a antiserum and the anti-Xpress antibody against an epitope in the His-tag of His-rabaptin4. Results are given in Figure 4(A) which shows that some rab4a is captured on the beads from the control rab4a CHO cells, probably due to the two histidine residues in rab4a. On co-expression of His-rabaptin4 the amount of co-precipitated rab4a increased severalfold. Because the association of rab4a and His-rabaptin4 is sensitive to non-ionic detergents, the amount of rab4a co-isolated with His-rabaptin4 using this method probably represents an underestimation.

As non-covalent complexes between rab4a and His-rabaptin4 dissociate in Laemmli sample buffer, they could not be detected in the previous experiment. We therefore repeated the co-precipitation assay in the presence of the thiol-cleavable cross-linker DTSP. Cells were pre-permeabilized with 0.05 % saponin to enhance their permeability to DTSP. Under these conditions His-rabaptin4 remained associated with rab4a-containing endosomes in non-fixed cells as ascertained by immunofluorescence microscopy. Post-nuclear supernatants prepared from the pre-extracted cells were incubated with Ni-NTA resin and washed as above. Proteins retained on the Ni-NTA beads were then separated by SDS/PAGE under reducing and non-reducing

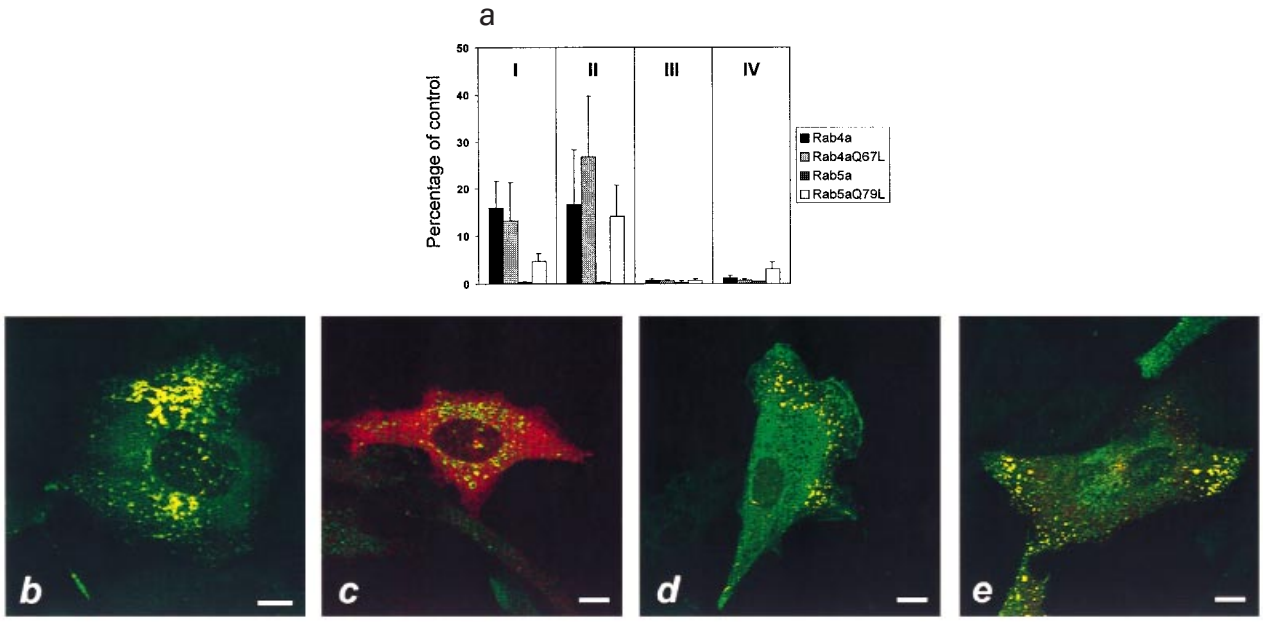


**Figure 5 Determination of the rab4a binding domain on rabaptin4**

Deletion constructs of rabaptin4 and rabaptin5 were co-transformed with rab4a, rab4aQ67L, rab5a or rab5aQ79L in YGH1. Interactions were quantitated in a liquid $\beta$-galactosidase assay, and normalized to the reporter activation of a transformant expressing the full-length GAL4 transcriptional activator. I, #16B; II, rabaptin4$\Delta$C; III, rabaptin4$\Delta$N; IV, rabaptin5$\Delta$N. Data points represent means $\pm$ S.D. of triplicates (**a**). CHO cells were transfected with each of the His-rabaptin4 domains and either rab4a or NHrab5a. In cells co-transfected with rab4a (green) and His-rabaptin4$\Delta$C (red), the two proteins colocalized extensively on dispersed perinuclear organelles (**b**). In cells co-transfected with rab4a (green) and His-rabaptin4$\Delta$N (red), His-rabaptin4$\Delta$N is not recruited to rab4a-containing endosomes and has a largely cytoplasmic distribution (**c**). In contrast, when NHrab5a (green) was co-transfected with either His-rabaptin4$\Delta$C (**d**, red) or His-rabaptin4$\Delta$N (**e**, red), the rabaptin4 domains are recruited to NHrab5a-containing endosomes in the peripheral cytoplasm. Bars represent 10 $\mu$m.

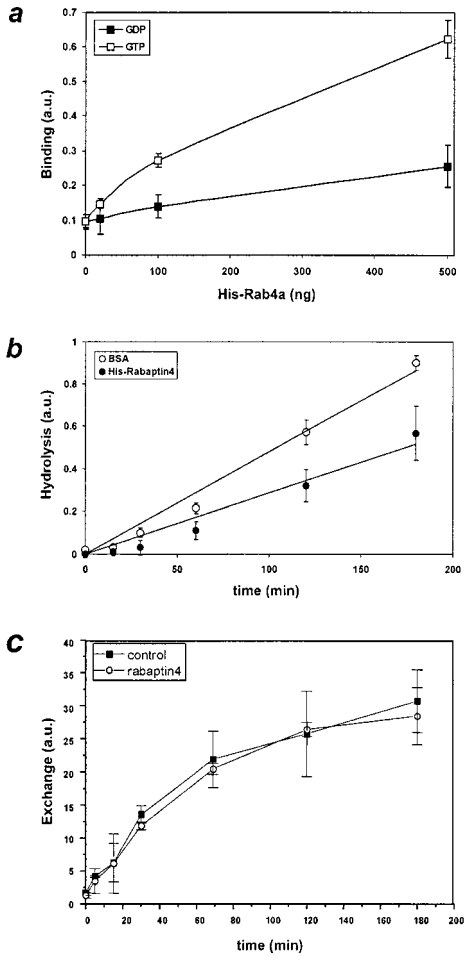


**Figure 6 Effect of His-rabaptin4 on His-rab4a GTPase activity**

His-rabaptin4ΔC was immobilized in a microtitre plate and incubated with His-rab4a in the presence of GDP or GTP. Binding was detected using anti-rab4a antibodies and a horseradish peroxidase-conjugated secondary antibody. An approx. 5-fold increase in binding was observed in the presence of GTP compared with GDP, showing that the interaction preferred the GTP-bound conformation of His-rab4a. When wells were coated with Blotto instead of His-rabaptin4ΔC, the signal was constant for both rab4GDP and rab4GTP and equal to 0.30. This absorbance value was subtracted from the data points (**a**). [$\gamma$-$^{32}$P]GTP-loaded His-rab4a was incubated with His-rabaptin4ΔC, or BSA for different periods of time. In the presence of His-rabaptin4ΔC the intrinsic rate of GTP-hydrolysis was reduced by 45% as compared with the incubations with BSA (**b**). GDP-loaded His-rab4a was incubated with 1 $\mu$M [$^{35}$S] guanosine 5′-[$\gamma$-thio]triphosphate ($3.7 \times 10^6$ Bq/mmol) for different periods of time at 30 °C in the presence or absence of a 10-fold molar excess of His-rabaptin4ΔC. No effect was observed on the rate of guanine nucleotide exchange on His-rab4a (**c**).

conditions, followed by Western blotting. A high-$M_r$ complex containing rab4a was isolated under non-reducing conditions from the double transfectants as shown in Figure 4(B), but not from the control cells transfected with rab4a only. The weak signal of the complex was most likely due to partial or complete masking of the rab4 and Xpress (results not shown) epitopes respectively. Upon reduction with $\beta$-mercaptoethanol, the complex was disrupted and rab4a and His-rabaptin4 were detected at $M_r \sim 24000$ and $\sim 100000$ respectively. Since the apparent $M_r$ of the complex was $> 130000$, it either consisted of more than one molecule of rab4a and His-rabaptin4, or contained additional unidentified proteins required for rab4a function. In support of this, two-hybrid assays revealed that rabaptin4 bound to itself, rabaptin5, and to other proteins (results not shown).

## Rab4a binds the N-terminus of rabaptin4

Since both rab4a and rab5a interacted with #16B, we next started to establish their binding domains on rabaptin4 using yeast two-hybrid assays. As shown in Figure 5(a), rabaptin4ΔN (amino acid residues 469–830) did not bind to any of the rab constructs tested, whereas rabaptin5ΔN (amino acid residues 469–863) interacted with rab5aQ79L, but not with rab5a, rab4a, or rab4aQ67L. Rabaptin4ΔC (amino acid residues 11–388) readily interacted with rab4a and rab4aQ67L, but surprisingly also with rab5aQ79L. We then analysed the association of the rabaptin deletion constructs with rab4a and rab5a using confocal immune fluorescence microscopy. In His-rabaptin4ΔC/rab4a transfectants, we observed extensive co-localization between His-rabaptin4ΔC and rab4a on the structures shown in Figure 5(b), In contrast, in His-rabaptin4ΔN/rab4a transfectants, His-rabaptin4ΔN was distributed in the cytoplasm (Figure 5c). Importantly, His-rabaptin4ΔC is recruited to more dispersed, peripherally localized rab4a-containing organelles that were distinct from those seen in Figure 3(c). We concluded, therefore, that although the C-terminal region of rabaptin4 does not bind to rab4a, it contained information required for proper targeting to the perinuclear rab4a-containing recycling endosomes. In His-rabaptin4ΔC/NHrab5a transfectants, we also observed recruitment of His-rabaptin4ΔC to the peripherally localized NHrab5a structures (Figure 5d). A similar staining pattern was seen in cells expressing NHrab5a and His-rabaptin4ΔN (Figure 5e). Thus, although rab5a interacted poorly with rabaptin4 in two-hybrid assays, we confirmed the presence of a rab5a-binding site in the C-terminal half of the protein, and identified a novel rab5a-binding site in the N-terminal half of the protein by immunofluorescence microscopy and two-hybrid assays. Rab4a associated with one binding site in the N-terminal half of rabaptin4.

## Rabaptin4 directly binds rab4a–GTP and inhibits its intrinsic GTPase activity

To show that rabaptin4 binds directly to rab4a we developed an *in vitro* binding assay using recombinant proteins. His-rabaptin4ΔC was immobilized in a microtitre plate and incubated with increasing amounts of His-rab4a, either in the presence of GDP or GTP. As shown in Figure 6(a), rab4a binding to rabaptin4 was concentration- and nucleotide-dependent, with $\sim$5 fold preference of GTP over GDP. Therefore the interaction of rab4a with rabaptin4 is direct and did not require other factors. Since it is thought that effectors stabilize GTPases in their GTP conformation, we next investigated the effect of rabaptin4 on rab4a–GTP. Recombinant His-rab4a was pre-loaded with [$\gamma$-$^{32}$P]GTP and incubated with His-rabaptin4ΔC, or the same concentration of BSA. Previously it was shown that low concentrations of BSA do not affect GTP-hydrolysis-rate measurements [24]. As shown in Figure 6(b), His-rabaptin4ΔC reduced the GTP-hydrolysis rate of His-rab4a. Curve-fitting analysis revealed that the rate constant of GTP hydrolysis was reduced from 0.0046 min$^{-1}$ to 0.0026 min$^{-1}$ in the presence of His-rabaptin4ΔC. A similar effect has been reported for the rab9 effector p40 on the GTP hydrolysis rate of rab9 [4]. The reduction of the intrinsic GTPase activity of His-rab4a was specific for His-rabaptin4, since it was not observed in the presence of BSA. To investigate whether or not rabaptin4 enhanced guanine nucleotide exchange, we next performed guanine nucleotide exchange reactions on rab4a in the presence or absence of His-rabaptin4ΔC. As shown in Figure 6(c), His-rabaptin4ΔC does not influence guanine nucleotide exchange on His-rab4a. Thus

rabaptin4 acts as a true effector of rab4a with respect to the stabilization of its GTP-bound form.

## DISCUSSION

Small GTPases of the rab family play a critical role in membrane traffic. Rab proteins are specifically associated with the cytoplasmic face of intracellular organelles, where the GTP-bound form plays a mechanistic role in vesicle docking and fusion that is not fully understood. Recent evidence suggests that rab GTPases in their GDP-bound form may be involved in vesicle budding [25]. Regulation of the activities of the GDP form at the donor compartment, and the GTP form at the acceptor site, may provide a control mechanism to regulate the exit of membrane and cargo from the donor organelle by the spatial organization of a rabGTPase. We previously showed that rab4a is associated with early endosomes and recycling vesicles and that it is involved in the regulation of transport in the recycling pathway from sorting endosomes to the plasma membrane [16]. As recycling vesicles from early endosomes may either directly fuse with the plasma membrane or be targeted in parallel with the perinuclear recycling compartment, it has been difficult to assess which of the two pathways is controlled by rab4a. Conceivably, blocking either one of them by overexpression of rab4a or dominant negative mutants might be compensated by shunting transport in the other route, explaining the relatively mild endocytosis phenotype observed after rab4a overexpression. The fact that rabaptin4 stabilized rab4a on recycling endosomes and because we could not detect rab4a by immunogold electron microscopy on the plasma membrane [26], suggests that rab4a acts between sorting endosomes and recycling endosomes.

We report here the characterization of rabaptin4, a novel protein functionally interacting with rab4a–GTP. The cDNA sequence of rabaptin4 is very similar to that of rabaptin5, with the exception of an in-frame deletion of 33 amino acid residues in the C-terminal region of the protein. Strikingly, the identical deletion is present in rabaptin5$\beta$, giving it a higher identity with rabaptin4 than rabaptin5. Since the deletion is immediately adjacent to the rab5a binding site in rabaptin5 and rabaptin5$\beta$, and because rabaptin5$\beta$ is a less potent effector than rabaptin5 in homotypic early-endosome fusion [27], this internal deletion possibly modulates binding of rab5a with the effector molecule. Importantly, rabaptin4 is not a splice variant of rabaptin5, since intron sequences were not present in the amplification product obtained from genomic DNA. Thus rabaptin4 is the third rabaptin protein that has been identified, documenting that there may be a family of rabaptins interacting with specific subsets of rabGTPases. Our RT-PCR analyses indicated that the rabaptin5 message appears to be more abundant than that of rabaptin4. As rabaptin5 contains at least one internal splice site outside of the region that is amplified in the duplex RT-PCR assay, it is possible that the stronger rabaptin5 band (Figure 2) is partially caused by amplification of rabaptin5 isoforms.

In two independent assays we established that the identical rabaptin4 and rabaptin5 N-termini contain a rab5a-binding site. The novel N-terminal rab5a binding domain has not been appreciated before [10] and may have important mechanistic implications for the regulation of membrane transport through early endosomes. It was postulated that rabaptin5, by binding rab4a at its N-terminus and rab5a at its C-terminus, may act to co-ordinate the activities of the two endosomal rab proteins. Now that we found that both rabaptin4 and rabaptin5 do bind rab5a to their N-termini, a mechanistically different scenario is possible in which rab4a and rab5a may compete for a mutual binding domain or in which they influence each other's binding to the N-terminus of either rabaptin. Given the fact that rab5a (but not rab4a) is also present at the plasma membrane and on coated vesicles, it is equally possible that different rab5a-binding domains on the rabaptins are used at distinct intracellular locations of rab5a. Thus, irrespective of the question whether rabaptin4 and rabaptin5 have similar functions, the fact remains that both rabaptins have two binding sites for rab5a. The presence of two separate rab5a binding sites is not a unique property of rabaptin effector molecules. Similarly, EEA1, another rab5a effector also has two rab5a-binding domains distributed over N- and C-terminal regions of the molecule [6]. Unlike rabaptin4 and rabaptin5, EEA1, however, does not interact with rab4a [10] and its function so far appears to be restricted to sorting endosomes.

Our data suggest that rab4a–GTP may act as a docking site for rabaptin4 and that rabaptin4 stabilizes rab4a–GTP on its target compartment. Because rabaptin4 binds to rab4a–GTP, we reasoned that co-expression of rab4a and rabaptin4 might provide information on the target organelle of rab4a–GTP-containing recycling vesicles. Indeed in rabaptin4/rab4a and rabaptin4/rab4aQ67L double transfectants, co-expression of the two proteins led to the expansion of a perinuclear compartment enriched in cellubrevin and internalized Cy3-Tf. The location of this organelle and the enrichment of cellubrevin and Cy3-Tf are hallmarks of the perinuclear recycling compartment [28,29]. We previously showed in pulse–chase experiments that FITC-Tf accumulated in this compartment after it had traversed rab4a-containing endosomes. Together with the present results, this suggests that the recycling compartment appears to be the target for rab4a-containing transport vesicles and not the plasma membrane. A rab4a–rabaptin4 complex on the perinuclear recycling compartment might provide a docking site for other proteins and assist in the fusion of recycling vesicles with the perinuclear recycling compartment. The fact that rab4a and rabaptin4 can be cross-linked in a high-$M_r$ complex is consistent with this hypothesis. Other rab GTPases including Sec4p [30] and rab5a [9] are also known to be present in hetero-oligomeric complexes. Intrinsic GTP hydrolysis on rab4a, or the recruitment of a GAP to the rab4a–rabaptin4 complex might convert rab4a into the GDP-form which initiates the dissociation of the complex, since rab4aGDP no longer binds to rabaptin4. Tuberin was shown to be a candidate rabGAP [30], although its specificity towards different rab proteins has not been rigorously evaluated. In agreement with the scaffold function of an endosomal rab–rabaptin complex, tuberin also binds to rabaptin5 [31], suggesting a role for rabaptins in the recruitment of GAP proteins.

An important question that remains to be solved is why the cell employs two distinct rabaptins each with the ability to bind rab4a and rab5a, to control vesicular transport to and from early endosomes. One scenario involves the recruitment of rabaptin5 by rab5aGTP to facilitate docking of incoming coated vesicles with early endosomes. After or during fusion, the rab5a–rabaptin5 complex might recruit rabaptin4 through interactions between the coiled-coil regions of rabaptin5 and rabaptin4. The locally concentrated rabaptin4 molecules might next be recruited to rab4a-containing vesicles to execute their function in rab4a-dependent recycling from early endosomes. This model would be in agreement with the partially overlapping distributions of rab5a and rab4a on early endosomes.

We thank Jim Bischoff, Philippe Chavrier, Thierry Galli, Marino Zerial, Bruno Goud, Graham Warren, Jeanette Leusen, Rachel Leckie and Marcel Spaargaren for generously providing reagents and our colleagues at the Department of Cell Biology for helpful suggestions. This work was supported by grants from the Netherlands Organization for Medical Research and the Dutch Cancer Society to P. van der S., who is an investigator of the Royal Netherlands Academy of Arts and Sciences.

## REFERENCES


1 Olkkonen, V. and Stenmark, H. (1997) Int. Rev. Cytol. **126**, 1–85
2 Pfeffer, S. R. (1999) Nat. Cell Biol. **1**, E17–E22
3 Wang, Y., Okamoto, M., Schmitz, F., Hofman, K. and Südhof, T. C. (1997) Nature (London) **388**, 593–598
4 Diaz, E., Schimmoller, F. and Pfeffer, S. R. (1997) J. Cell Biol. **138**, 283–290
5 Stenmark, H., Vitale, G., Ullrich, O. and Zerial, M. (1995) Cell **83**, 423–432
6 Simonsen, A., Lippe, R., Christoforidis, S., Gaullier, J. M., Brech, A., Callaghan, J., Toh, B. H., Murphy, C., Zerial, M. and Stenmark, H. (1998) Nature (London) **394**, 494–498
7 Ren, M., Zeng, J., Chiarandini, C., Rosenfeld, M., Adesnik, M. and Sabatini, D. D. (1996) Proc. Natl. Acad. Sci. U.S.A. **93**, 5151–5155
8 Echard, A., Jollivet, F., Martinez, O., Lacapere, J. J., Rousselet, A., Janoueix-Lerosey, I. and Goud, B. (1998) Science **279**, 580–585
9 Horiuchi, H., Lippe, R., McBride, H. M., Rubino, M., Woodman, P., Stenmark, H., Rybin, V., Wilm, M., Ashman, K., Mann, M. and Zerial, M. (1997) Cell **90**, 1149–1159
10 Vitale, G., Rybin, V., Christoforidis, S., Thornqvist, P. O., McCaffrey, M., Stenmark, H. and Zerial, M. (1998) EMBO J. **17**, 1941–1951
11 Rybin, V., Ullrich, O., Rubino, M., Alexandrov, K., Simon, I., Seabra, M., Goody, R. and Zerial, M. (1996) Nature (London) **383**, 266–269
12 Bucci, C., Parton, R., Mather, I., Stunnenberg, H., Simons, K. and Zerial, M. (1992) Cell **70**, 715–728
13 Ullrich, O., Reinsch, O., Urbe, S., Zerial, M. and Parton, R. (1996) J. Cell Biol. **135**, 913–924
14 Chen, W., Feng, Y., Chen, D. and Wandinger-Ness, A. (1998) Mol. Biol. Cell **9**, 3241–3257
15 van der Sluijs, P., Hull, M., Zahraoui, A., Tavitian, A., Goud, B. and Mellman, I. (1991) Proc. Natl. Acad. Sci. U.S.A. **88**, 6313–6317
16 van der Sluijs, P., Hull, M., Webster, P., Goud, B. and Mellman, I. (1992) Cell **70**, 729–740
17 Chavrier, P., van der Sluijs, P., Mishal, Z., Nagelkerken, B. and Gorvel, J. P. (1997) Cytometry **29**, 41–49
18 Bottger, G., Nagelkerken, B. and van der Sluijs, P. (1996) J. Biol. Chem. **271**, 29191–29197
19 Galli, T., Chilcote, T., Mundigl, O., Binz, T., Niemann, H. and De Camilli, P. (1994) J. Cell Biol. **125**, 1015–1024
20 Nagelkerken, B., Mohrmann, K., Gerez, L., van Raak, M., Leijendekker, R. L. and van der Sluijs, P. (1997) Electrophoresis **18**, 2694–2698
21 Spaargaren, M. and Bisschoff, J. R. (1994) Proc. Natl. Acad. Sci. U.S.A. **91**, 12609–12613
22 Kabcenell, A. K., Goud, B., Northup, J. K. and Novick, P. J. (1990) J. Biol. Chem. **265**, 9366–9372
23 Lupas, A., Van Dyke, M. and Stock, J. (1996) Science **252**, 1162–1164
24 Shapiro, A. D., Riederer, M. A. and Pfeffer, S. R. (1993) J. Biol. Chem. **268**, 6925–6931
25 McLaughlan, H., Newell, J., Morrice, N., Osborne, A., West, M. and Smythe, E. (1998) Curr. Biol. **8**, 34–45
26 de Wit, H., Lichtenstein, Y., Kelly, R., van der Sluijs, P. and Klumperman, J. (1999) Mol. Biol. Cell. **10**, 4163–4176
27 Gournier, H., Stenmark, H., Rybin, V., Lippe, R. and Zerial, M. (1998) EMBO J. **17**, 1930–1940
28 Daro, E., van der Sluijs, P., Galli, T. and Mellman, I. (1996) Proc. Natl. Acad. Sci. U.S.A. **93**, 9559–9564
29 Ghosh, R. N., Mallet, W. G., Soe, T. T., McGraw, T. E. and Maxfield, F. R. (1998) J. Cell Biol. **142**, 923–936
30 TerBush, D. R., Maurice, T., Roth, D. and Novick, P. (1996) EMBO J. **15**, 6483–6494
31 Xiao, G. H., Shoarinejad, F., Jin, F., Golemis, E. and Yeung, R. S. (1997) J. Biol. Chem. **272**, 6097–6100


Received 20 August 1999/11 November 1999; accepted 4 January 2000